


RESEARCH ARTICLE

Changes in the fraction of strongly attached cross bridges in mouse atrophic and hypertrophic muscles as revealed by continuous wave electron paramagnetic resonance

Laura Galazzo,¹ Leonardo Nogara,² Francesca LoVerso,² Antonino Polimeno,¹ Bert Blaauw,² Marco Sandri,^{2,3}  Carlo Reggiani,³ and  Donatella Carbonera¹

¹Department of Chemical Sciences, University of Padova, Padua, Italy; ²Venetian Institute of Molecular Medicine, Padua, Italy; and ³Department of Biomedical Sciences, University of Padova, Padua, Italy

Submitted 1 November 2018; accepted in final form 15 February 2019

Galazzo L, Nogara L, LoVerso F, Polimeno A, Blaauw B, Sandri M, Reggiani C, Carbonera D. Changes in the fraction of strongly attached cross bridges in mouse atrophic and hypertrophic muscles as revealed by continuous wave electron paramagnetic resonance. *Am J Physiol Cell Physiol* 316: C722–C730, 2019. First published March 13, 2019; doi:10.1152/ajpcell.00438.2018.—Electron paramagnetic resonance (EPR), coupled with site-directed spin labeling, has been proven to be a particularly suitable technique to extract information on the fraction of myosin heads strongly bound to actin upon muscle contraction. The approach can be used to investigate possible structural changes occurring in myosin of fibers altered by diseases and aging. In this work, we labeled myosin at position Cys707, located in the SH1-SH2 helix in the myosin head cleft, with iodoacetamide spin label, a spin label that is sensitive to the reorientational motion of this protein during the ATPase cycle and characterized the biochemical states of the labeled myosin head by means of continuous wave EPR. After checking the sensitivity and the power of the technique on different muscles and species, we investigated whether changes in the fraction of strongly bound myosin heads might explain the contractile alterations observed in atrophic and hypertrophic murine muscles. In both conditions, the difference in contractile force could not be justified simply by the difference in muscle mass. Our results showed that in atrophic muscles the decrease in force generation was attributable to a lower fraction of strongly bound cross bridges during maximal activation. In contrast in hypertrophic muscles, the increase in force generation was likely due to several factors, as pointed out by the comparison of the EPR experiments with the tension measurements on single skinned fibers.

atrophy; EPR; hypertrophy; tension

INTRODUCTION

Skeletal muscle is a highly plastic tissue, as its fibers can change their size and their functional properties to perform new tasks or respond to new conditions (for a review, see Ref. 6). The adaptive changes of muscle fibers occur in response to variations in the pattern of neural stimulation, loading conditions, availability of substrates, and hormonal signals. In response to increased functional demands, skeletal muscle fibers can increase their size (hypertrophy), while reduced activity leads to a decrease of cellular volume (atrophy). Although, as

general rule, the ability to generate force during contraction varies in proportion to muscle fiber cross-sectional area (CSA) (8, 12), there are notable examples of dissociation between force generation and fiber size. Both in human and in murine muscles, atrophy, either due to disuse (29, 32) or to aging (see Ref. 17 for a review), is accompanied by a decrease in specific tension. In our previous works, we found a dissociation between variations of muscle fiber size and force generation during maximal isometric contraction in some transgenic mouse models where muscle fiber size is modified by genetic manipulation of the signaling pathways controlling protein synthesis or degradation. In Akt-overexpressing muscle fibers, we observed an increase in active force well above the increase of fiber size (5). The opposite, i.e., a decrease in active force greater than the decrease of fiber CSA was observed in muscle fibers where *Atg7* gene was inactivated (9). It is worth to underline that, in view of its central position in the pathway regulating protein synthesis in the ribosomes, the overexpression of a constitutive active form of Akt is expected to induce protein accumulation and muscle fiber hypertrophy (19, 26). The impact of *Atg7* knockout, on the contrary, is less obvious, as *Atg7* is an essential component of the autophagy mechanism, i.e., a mechanism of protein degradation, and both increase and decrease of *Atg7* are followed by muscle fiber atrophy (16).

The force developed by skeletal muscle fibers maximally activated in isometric conditions recognizes two major determinants, the force generated by a single myosin motor and the number of myosin motors generating force at a given time. Electron paramagnetic resonance (EPR), coupled with site-directed spin labeling (1, 2, 7), can be an extremely useful tool to obtain reliable information on the number of cross bridges formed in muscle fibers during contraction. Thanks to the presence of one or more cysteines in the system of interest, in fact, it is possible to covalently attach a probe carrying a paramagnetic moiety that can be used as a conformational reporter of myosin during the ATP cycle. In continuous wave (CW)-EPR, the sample is inserted in a static magnetic field and it is continuously irradiated with microwaves at a fixed frequency. The absorption of such microwaves leads to the detection of an EPR signal, characterized by a line shape that reflects the mobility of the spin probe at the labeled site.

Due to the reorientation of the myosin head with respect to the actin filament, the spectra of the different biochemical

Address for reprint requests and other correspondence: D. Carbonera, Dept. of Chemical Sciences, Univ. of Padova, Via F. Marzolo 1, 35131 Padua, Italy (e-mail: donatella.carbonera@unipd.it).

states (i.e., rigor, relaxation, and contraction) will present characteristic line shapes that can be used to determine the fraction of myosin heads in the strong-binding state upon muscle contraction (21).

This type of analysis has been adopted before to investigate possible variations in the formation of the cross bridges in relation to aging and dysfunctions (13, 14) and oxidative stress (23) to assess or exclude the involvement of myosin structural changes in the variation of contractile power. Cysteine 707, which corresponds to SH1 of the SH1-SH2 helix, is located in the myosin head in a critical position for the chemomechanical transduction and has been proven to be a suitable site for site-directed spin labeling. Once labeled with a spin probe as 4-(2-iodoacetamido)-2,2,6,6-tetramethyl-1-piperidinyloxy spin label (IASL), this residue becomes diagnostic of myosin conformational changes with respect to the actin filament during muscle contraction. The residue is buried in the structure and has an accessible surface area of 12 Å to the solvent (24). The spin probe of choice for this spectroscopic investigation is 4-(2-iodoacetamido)-2,2,6,6-tetramethyl-1-piperidinyloxy spin label (3) instead of the most commonly used (1-oxyl-2,2,5,5-tetramethylpyrrolidine-3-methyl)methanethiosulfonate spin label (4) due to the treatment of the fibers with the reducing agent dithiothreitol (DTT) that would cause the release of the spin probe MTSL from the protein (11).

The EPR line shape of the spectrum of spin label at position 707 is affected by the orientation of the fibers with respect to the magnetic field and, most interestingly, by the different biochemical states of the protein during the ATP binding and hydrolysis cycle (i.e., rigor, contraction, and relaxation) (27, 30, 31). Thus the information that can be extracted from the EPR spectra is very precious to understand if differences in the force generation are due to a change in the number of attached cross bridges. In fact, the power of EPR consists of the possibility to place a probe selectively on myosin head and, by characterizing its behavior, to measure the capability in cross-bridge formation in altered and control systems.

On this ground we sought to exploit EPR resolution power to assess the fraction of attached cross bridges during maximal isometric contraction in skeletal muscle fibers of wild-type mice and of those mutants where variations of force and variations of fiber size are discordant.

Since mouse muscles are less studied than rabbit (21) and rat muscles (13), we first extended the analysis to a comparison between different species and then we focused on the two murine mutant muscle fibers. The experimental protocol and the method of analysis have been implemented in rabbit psoas fibers (21) and then applied to rat muscle fibers (13) and only in one study (14) to murine extensor digitorum longus (EDL) muscle preparation. For this reason, we decided to validate the selected experimental approach comparing EPR spectra of rabbit psoas fibers, with murine EDL and tibialis anterior and even with a very small bundle of human fibers.

MATERIALS AND METHODS

Muscle sample collection and preparation of muscle fiber bundles. EPR and mechanical measurements were carried out on single fibers or fiber bundles of mouse, rabbit and human muscles. Mouse muscle sampling was carried out according to the project approved by the Italian Ministero della Salute, Ufficio VI (Authorization No. C65) for Atg7 knockout (9) and according to project approved by local ethical

committee for Akt overexpression (5). Mice used in this work were euthanized according to the protocols approved by the Institutional Animal Care and Use Committee (Organismo Per il Benessere Animale). Rabbit muscles were derived as residual material from the project approved by the University of California, San Francisco Institutional Animal Care and Use Committee No. AN108976-02 (20). Human muscles were obtained as residual material from the project approved by the Ethics Committee of the University of Padua, Department of Biomedical Sciences (HEC-DSB08/16, see Ref. 18).

Generation of conditional inducible Akt transgenic mice was achieved, as previously described (5), by crossing a transgenic line that expresses the Cre recombinase under a muscle-specific (myosin light chain 1 fast) promoter with a second line that expresses Akt1 only after the deletion of an upstream DNA sequence by the Cre recombinase. In this model, the Akt coding sequence is fused to a modified estrogen receptor-binding domain; as a consequence, Akt phosphorylation and activation were induced only by exogenous treatment with tamoxifen, which binds the estrogen receptor. After one injection, Akt remains phosphorylated for 48 h. Thus mice received intraperitoneum 1 mg of tamoxifen once every other day. Treatment was carried out in adult 5- to 6-mo-old animals, and muscle sampling was performed after 3 wk.

Generation of conditional inducible Atg 7 knockout mice was achieved as described in Ref. 16 by crossing mice bearing an *Atg7* flox allele (*Atg7^{flox}*) with transgenic mice expressing *Cre* under the control of a myosin light chain 1 fast promoter as described in Ref. 9. In this study, a comparison between healthy and atrophic mice has been carried out at two different ages; more precisely, 15- and 26-mo-old animals were analyzed.

In all EPR experiments, fiber bundles were dissected in a skinning solution composed of 120 mM potassium acetate (P1190), 50 mM MOPS (M1254), 5 mM EGTA (E3889), 5 mM magnesium acetate (M5661), 5 mM DTT (D0632), and 50% glycerol (G9012), pH adjusted to 7.0 (25). All the chemicals used for sample preparation described in this section and in *Labeling at C707 (SH1)* were purchased from Sigma-Aldrich. The catalog numbers are indicated in parenthesis. After the dissection, muscles were tied to wood or plastic sticks with a silk thread to keep them stretched and to facilitate the rigor state.

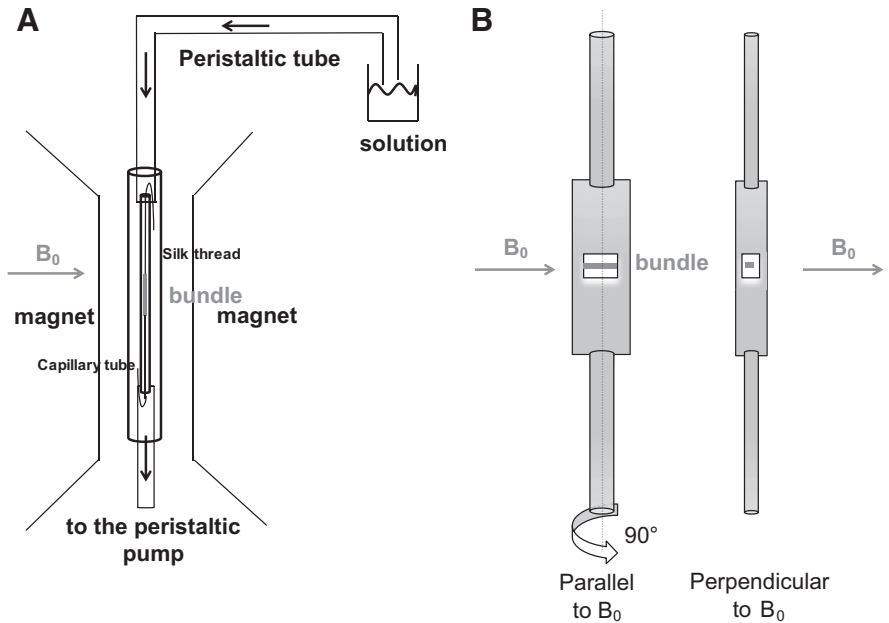
Muscle fiber bundles were kept at 4°C for 3 days under mild stirring, and fresh skinning solution was provided every 24 h. After this period, muscles were stored at -20°C in a 50% glycerol rigor solution [see *Labeling at C707 (SH1)* for the composition of the rigor buffer] plus DTT 5 mM until the day of use.

In experiments aimed to measure tension development in skinned single fibers, the bundles were immersed in skinning solution with 50% glycerol at -20°C.

Labeling at C707 (SH1). The labeling procedure, which has been proven to be selective for C707, was the same used by Ostap and coworkers (21).

All the operations were carried out at 4°C under mild stirring and all the washes were carried out for 5 min. In the first step, fibers were washed twice in a rigor buffer (RB: potassium acetate 120 mM, MOPS 50 mM, EGTA 1 mM and magnesium acetate 5 mM, pH 7.0) to remove glycerol, then washed for 15 min in RB containing Triton X-100 (X100) 0.5% vol/vol, to solubilize lipids and proteins. The detergent was then removed by two washes in RB, and fibers were incubated for 60 min in RB containing DTNB (D8130; 60 μM); this preblocking step is aimed to block the non-SH1 thiols (as for example the reactive Cys 697) and therefore to allow the selective labeling of C707, as the latter is not accessible in rigor state and it is not blocked. Two washes in RB were then carried out to remove the residual DTNB and then fibers were relaxed with two washes in RB plus tetra-potassium pyrophosphate (K₄PP_i; 10 mM), to make the desired cysteine become reactive. C707 was then labeled by incubation for 60 min in the same buffer of the previous wash with the addition of IASL (253367) 500 μM. The specificity of the labeling is assured by the fact

Fig. 1. *A*: schematic representation of the setup used for continuous wave-electron paramagnetic resonance (CW-EPR) measurements in continuous flow of solution. *B*: schematic representation of the homemade flat cell used for CW-EPR orientation measurements with indication of field of sample orientation with respect to the magnetic field.



that all the other thiols are blocked. Fibers were then washed twice in RB plus K_4PP_i , twice in RB, and finally incubated with the reducing agent DTT (10 mM) for 15 min to unblock the other thiols. At the end of the procedure, fibers were washed twice in RB, three times in RB + 50% glycerol, and finally stored at -20°C until the EPR measurements were carried out.

Spectroscopic measurements. For EPR determination of the different biochemical states, bundles of fibers (~100–150 fibers each, ~8- to 10-mm long and 0.2-mm thick) prepared as described above were tied on both sides with a silk thread, while immersed in RB, and then transferred into a clear fused quartz capillary tube (internal diameter: 0.9 mm) that was closed on both sides with a silicon tube. The capillary and the tubes were then inserted in a 2×3 EPR tube that was located in the cavity (Bruker ER4103TM) of the EPR instrument. In this conformation, the fibers were in a perpendicular configuration with respect to the magnetic field direction. On one side, the silicon tube ended in a beaker containing the desired solution (rigor, relaxing or activating), while on the other side the other silicon tube was connected to a peristaltic pump that enabled the continuous flow of fresh solution during the whole experiment. The speed of the pump was set to 0.5 ml/min. The bundle was gently elongated at 1.1 slack length while immersed in relaxing solution and kept at that length for the whole duration of the experiment. The setup is shown in Fig. 1A.

For orientation measurements, small bundles of fibers were located in the well of a homemade plexiglass flat cell, as shown in Fig. 1B. The well was then closed with a thin cap, and the cell was inserted in the cavity of the EPR instrument in such a way that perpendicular and parallel orientations of the fibers with respect to the magnetic field could be obtained by simple rotation of the cell in the cavity.

CW-EPR measurements were carried out on a Bruker Elexsys E580-X-band spectrometer equipped with a ER4103TM cavity. Acquisition parameters were the following: temperature = 298 K; microwave frequency = 9.78 GHz; modulation frequency = 100 kHz; modulation amplitude = 0.5 mT; power attenuation = 15 dB; time constant = 20.48 ms; conversion time = 81.92 ms; and number of data points = 1,024. Spectra were acquired for 15 min in each biochemical state.

Composition of the solutions. For each fiber bundle EPR spectra were collected under conditions of rigor, relaxation, and contraction. To induce the three conditions, the following solutions were flowed over the fiber bundle: 1) rigor solution (RB); see *Labeling at C707*

(SH1); 2) relaxing solution: the composition was the same of the rigor solution, with the addition of 4 mM Na-ATP (A7699), 20 mM creatine phosphate (27920), and 200 U/ml creatine phosphokinase (C3755); and 3) contraction (or activating) solution: the composition was the same of the relaxing solution, with the addition of 2 mM $\text{CaCl}_2 \cdot 2\text{H}_2\text{O}$ (C8106).

Analysis of EPR spectra. Since the aim of the EPR recording and analysis was to determine the proportion of myosin heads in strong binding state, the analysis was focused on the low field region of the spectra. Previous studies have shown that this region is most sensitive to myosin head structural changes when C707 (SH1) is labeled with IASL (3, 13, 14). The portion of the spectra considered in the analysis is shown in Fig. 2 in the dotted square.

The analysis was based on the model proposed in several other works (see Refs. 13, 14, and 21 for an example) that assumes the

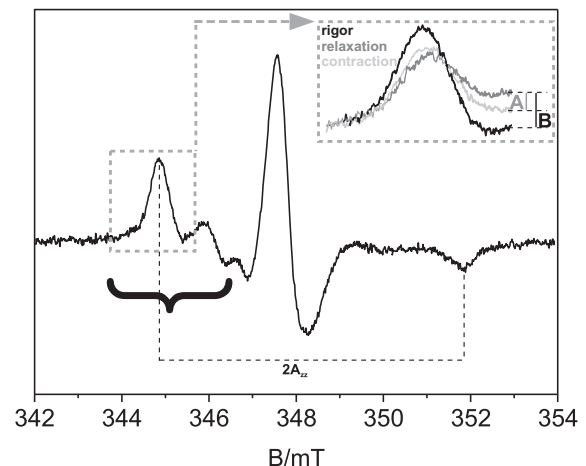


Fig. 2. Example of a continuous wave-electron paramagnetic resonance (CW-EPR) spectrum at room temperature of a bundle of fibers from rabbit psoas in rigor state. The low-field portion of the spectrum is highlighted within the curly bracket to clarify the region that is considered for the analysis and shown in RESULTS AND DISCUSSION. The $2A_{zz}$ value is discussed in the INTRODUCTION. *Inset*: procedure used to determine the fraction x during contraction. See text for definitions of A and B.

spectra obtained during contraction result from a linear combination of the spectra recorded in rigor where all cross bridges are assumed to be in strongly bound state and in relaxation where all cross bridges are in weak binding state. On this basis, it is possible to quantify the portion of myosin heads in weak and strong structural state in contraction state. Thus considering Eq. 1:

$$V_{\text{con}} = xV_{\text{rig}} + (1 - x)V_{\text{rel}} \quad (1)$$

where V_{rig} (rigor) corresponds to the CW-EPR signal intensity when all heads are in the strong binding structural state ($x = 1$) and V_{rel} (relaxation) corresponds to the intensity when all heads are in the weak-binding structural state ($x = 0$); the quantification is done solving x for each field position in the contraction spectrum as described in Eq. 2 and clarified in Fig. 2, *inset*:

$$x = (V_{\text{rel}} - V_{\text{con}}) / (V_{\text{rel}} - V_{\text{rig}}) = A/B \quad (2)$$

In this equation, every V corresponds to the intensity of the EPR signal at that field position for the biochemical state under investigation; the final averaged x value, representing the number of cross bridges, is given by averaging all the calculated x values on the number of points collected in the spectrum obtained by sweeping the magnetic field. Figure 2 also shows the parameter A_{zz} , principal value of the hyperfine tensor along the z-direction, which is half of the splitting between the positive low field peak and the negative high field peak of the CW spectrum. This parameter can be extracted from CW spectra at X-band in the rigid limit, as in the powder-like spectrum characterizing the rigor condition. An increase in the mobility of the nitroxide at the labeled site results in a decrease of the maximum splitting of the spectrum.

Statistical analysis. To have a statistical pool of measurements, all of the experiments (both for control and altered muscles) were carried out on muscles obtained from four different animals (two males and two females). For each muscle, five different bundles were analyzed. The fraction of strongly bound cross bridges x given in RESULTS is the average obtained from all the repetitions together with its standard deviation. All data are expressed as means \pm SD. Differences between groups were assessed using Student's *t*-test. Significance was defined as a value of $P < 0.05$ (95% confidence).

Tension measurements on single skinned fibers. Data on tension generation by single muscle fibers derive from previously published studies (5, 9). The protocol for fiber preparation and tension measurement can be summarized as follows. Fiber bundles stored in skinning solution with 50% glycerol at -20°C were transferred to skinning solution with ATP on the day of the experiment. Single fibers were manually dissected under a stereomicroscope ($\times 10$ – 60) and shortly bathed in skinning solution containing 1% Triton X-100 to ensure complete membrane permeabilization. Segments 1- to 2-mm long were then cut from the fibers, and light aluminum clips were applied at both ends. The solutions used had the following composition (in mM): 150 skinning solution: potassium propionate (CDS000543), 5 magnesium acetate, 5 Na-ATP, 5 EGTA, and 5 KH_2PO_4 (P5655); relaxing solution (in mM): 100 KCl (P9333), 20 imidazole (I5513), 5 MgCl_2 (M8266), 5 Na-ATP, and 5 EGTA; preactivating solution had a similar composition except that EGTA concentration was reduced to 0.5 mM, and 25 mM creatine phosphate and 300 U/ml creatine phosphokinase were added; and activating solution (pCa 4.6). The pH of all solutions was adjusted to 7.0 at the temperature at which solutions were used (12°C for Atg7 experiments and 20°C for Akt experiments). Protease inhibitors were present in all solutions. In each fiber segment, isometric tension (P_o) was measured during maximal activations at optimal sarcomere length (2.5 μm). Images of each fiber were taken with a camera connected with the microscope at $\times 360$. Cross-sectional area was calculated from the average of three diameters, spaced at equal intervals along the length of the fiber segment, assuming a circular shape.

RESULTS AND DISCUSSION

EPR measurements on muscle fibers of different species. We analyzed the CW-EPR spectra in rigor, relaxation, and contraction in different bundles of fibers, collected from mouse, rabbit, and human muscles. These experiments aimed to compare our protocols and the results of our analysis with those available in the literature for rabbit psoas (21) and mouse EDL (14) and to extend our analysis by exploring the behavior of mouse tibialis anterior and human vastus lateralis, as no EPR data on the different biochemical states of these muscles have been reported until now. While rabbit psoas and the two murine muscles (EDL and tibialis anterior) are composed by more than 90% of fast fibers, human vastus lateralis has a mixed composition with $\sim 50\%$ slow fibers (28). The results are presented in Fig. 3, where we show some records obtained in rabbit psoas (Fig. 3A), two different mouse muscles (EDL and tibialis anterior; Fig. 3, B and C), and a small bundle of a human vastus lateralis (Fig. 3D).

In Fig. 3, A–D, only the low-field portion of the CW-EPR spectrum is reported to highlight the differences in the line shapes in that region, which is the most sensitive to the myosin conformational changes. Due to the small size of residual fragment of human muscles, bundles of ~ 20 fibers were studied and the corresponding spectrum in Fig. 3D was recorded with a lower number of points in order to obtain an acceptable signal-to-noise ratio with acquisition times comparable to those used for the other samples.

The analysis of the spectra in Fig. 3 shows that, in the presence of ATP, the spin labels are more mobile with respect to myosin head than in rigor state; this evidence is given by the change in the maximum splitting of the spectrum $2A_{zz}$ (see Fig. 2) in the three different biochemical states: the greater this value, the more immobilized is the nitroxide. In fact, in relaxation conditions, we observed a decrease of ~ 0.25 mT in the $2A_{zz}$ value, while, in the presence of calcium, there was an increase of ~ 0.2 mT of the splitting in the spectrum, highlighting that a certain number of spin labels becomes more rigidly bound to myosin head upon contraction. The $2A_{zz}$ values have been determined directly on the recorded CW-EPR full-width spectra (not shown).

By using the approach described in MATERIALS AND METHODS, the fraction of strongly bound cross bridges (x) detected during contraction was calculated; for all the tested bundles the value varied between 0.35 and 0.4, depending on the different samples. This result suggests that, in the contraction state, the population of myosin heads in the strong-binding (force generating) structural state is between 35 and 40%, while the other 65–60% is in a weak-binding state, values close to those previously reported (13). Interestingly, the values of fraction of strongly attached myosin heads is comparable, taking into account the temperature difference, to that recently calculated with a completely different experimental approach in rabbit psoas fibers (22).

Our results on a tiny bundle of human muscle fibers confirm the sensitivity and the power of the technique for the scope of the study, as a reliable result can be obtained even with a very small amount of material. Moreover, the consistent values obtained in different biological systems encourage the investigation on possible alterations of the fraction of strongly

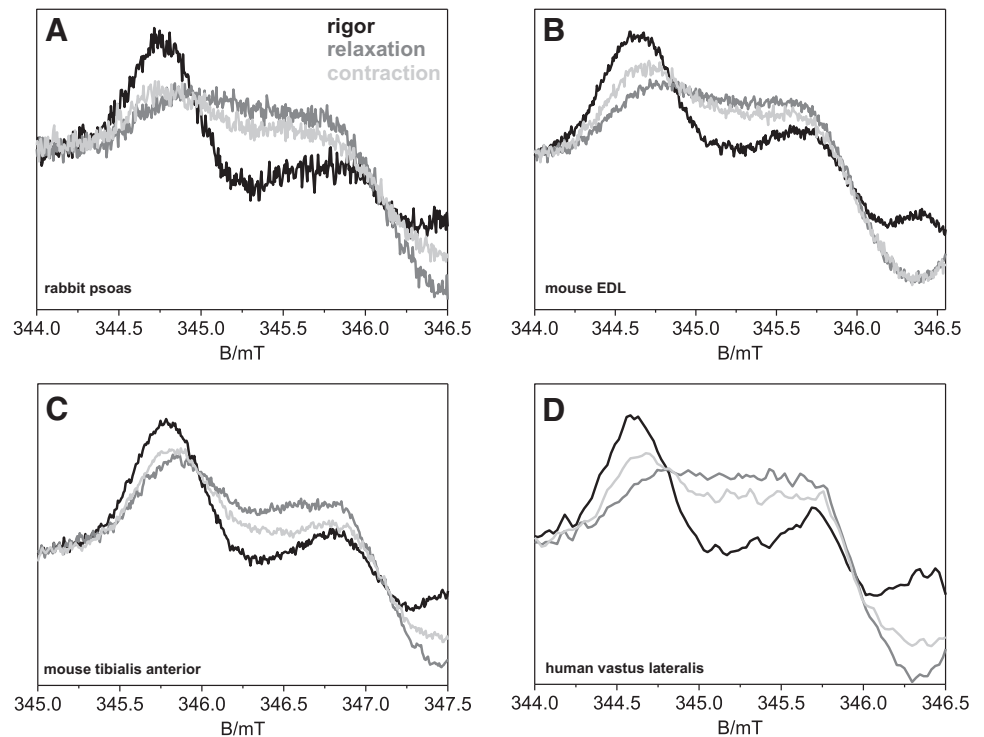


Fig. 3. Low-field portion of continuous wave-electron paramagnetic resonance (CW-EPR) spectra at room temperature of muscle fibers in rigor (black), relaxation (gray), and contraction (light gray) for rabbit psoas (A), mouse extensor digitorum longus (EDL; B), mouse tibialis anterior (C), and human vastus lateralis (D).

bound cross bridges in murine models where force generation is lower or higher than expected.

The fraction of strongly attached cross bridges in Atg7 knockout muscles. The autophagy pathway, together with the ubiquitin-proteasome pathway, represents a major route for protein degradation. It is, therefore, expected that an excessive activation of autophagy will be followed by muscle atrophy. However, a severe atrophy is also induced by the specific inhibition of autophagy in skeletal muscles achieved with conditional inducible knockout of the gene coding for Atg7, i.e., one of the essential components of the autophagy machinery (9, 16). The decrease in muscle fiber size is accompanied by a decrease in contractile performance, which can be detected *in vivo* as well as *in vitro* with mechanical experiments on single muscle fibers. As shown in our previous studies (9, 15), the decrease in force generated during maximal activation is greater than the decrease in fiber size, thus pointing to a reduction of specific force or tension. We could not document any change in fiber type composition (15) and in myofibrillar ultrastructure (9) sufficient to explain the loss in specific tension. Thus we adopted the EPR analysis of the mobility of IASL probe covalently attached to the cystein 707 (SH1) to assess whether the loss of ability to generate tension was due to a decreased fraction of attached cross bridges. The results are reported in Fig. 4.

To address possible age-related differences in atrophic muscles, we analyzed muscle fibers from mice of two different ages: in particular, we used 15-mo-old mice (which are considered as adult animals) and 26-mo-old mice (which are considered as old animals). In both cases, results were compared with control mice of the same age. In Fig. 4 on the left, spectra recorded on a control muscle fiber bundles are shown, while the corresponding knockout spectra are depicted on the right.

The values of the fraction x of myosin heads bound to actin during contraction are also reported in Fig. 4, as means \pm SD derived from the statistical analysis of the data obtained from the $n = 20$ repetitions performed for each of the four conditions considered (see MATERIALS AND METHODS). All the results are presented as the means \pm SD calculated over all the repetitions. Significance is defined as a value of $P < 0.05$ (95% confidence).

As mentioned in the MATERIALS AND METHODS, the analyzed bundles were taken from four different animals for every set of conditions (age and characteristics); for the statistical analysis, each sample was considered as an individual data point. However, no significant differences were found within muscles from the same animals; therefore, the standard deviation reflects the variability within different animals in the same conditions.

EPR spectra analysis enabled us to determine the fraction x of cross bridges in contraction for control and knockout samples at two different ages. For adult atrophic muscle fiber bundles, we found $x = 0.39 \pm 0.03$ for the control and $x = 0.30 \pm 0.02$ for knockout, corresponding to a significant decrease of $\sim 23\%$ in the fraction of strongly bound cross bridges (Fig. 4, A and B) and $x = 0.25 \pm 0.02$ for the control and $x = 0.21 \pm 0.01$ for knockout in old atrophic muscle fiber bundles, corresponding to a significant decrease of $\sim 16\%$ in the fraction of the strongly bound cross bridges (Fig. 4, C and D). The high number of repetitions and the very little variance encountered in these samples certify the statistical significance of the results.

It is worth pointing out that the fraction of the strongly bound cross bridges found in both the young and old control mice is in agreement with the one reported in the literature for similar samples (14). In addition, comparing the values in control muscles at the two different ages, we observed that

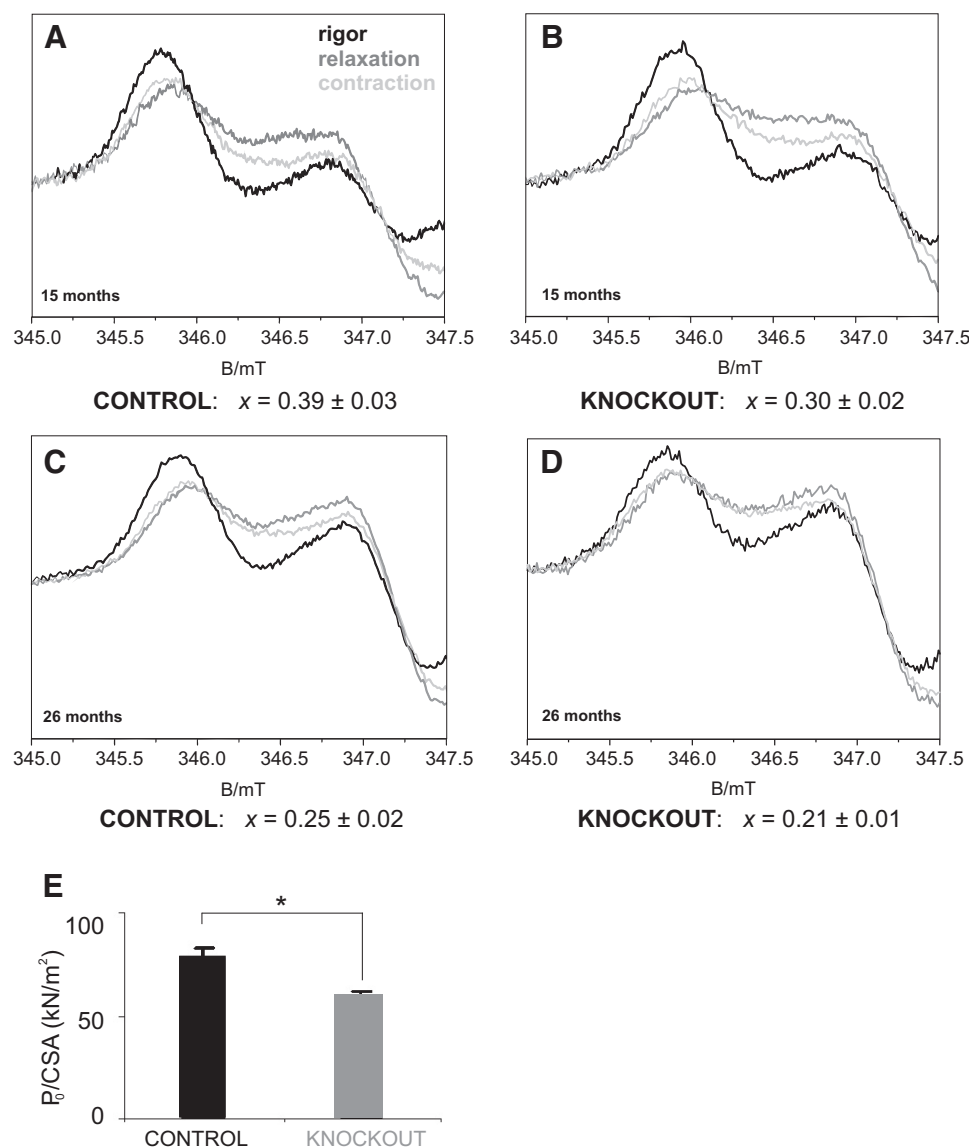


Fig. 4. Continuous wave-electron paramagnetic resonance (CW-EPR) spectra at room temperature on fiber bundles of mouse tibialis anterior muscle in rigor (black), relaxation (gray), and contraction (light gray) state. *A* and *C*: control muscles. *B* and *D*: *Atg7* knockout muscles. *A* and *B*: muscle fibers from 15-mo-old mice. *C* and *D*: muscle fibers from 26-mo-old mice. Values of the ratio x , indicating the proportion of strongly bound cross bridges are means \pm SD with $n = 20$ (equal number of bundles from 4 different animals, 2 males and 2 females). * $P < 0.05$, significant difference (95% confidence). *E*: tension measurements performed at 12°C on single skinned fibers corrected for the cross-sectional area. [Adapted from Carnio et al. (9); licensed under Creative Commons Attribution CC BY-NC-ND 3.0.]

there is a decrease in the fraction of attached cross bridges. This decrease is in agreement with similar results previously obtained in rat muscles (13).

Tension generation during maximal activation in optimal conditions (sarcomere length and free calcium concentration) as determined in our previous study (9) shows a decrease by 16% in old (26 mo) atrophic fibers compared with control fibers (Fig. 4E). The agreement between the fraction of cross-bridge reduction and the reduction of tension in skinned single fibers enabled us to conclude that the difference in force generation in atrophic mice can be exclusively ascribed to myosin and, more specifically, to a shift in the distribution of the relative percentages of the myosin head in the different structural states. Our previous observations (9) of an altered redox state in muscle fibers of *Atg7* knockout mice point to the oxidative posttranslational modification of the contractile proteins as the cause of the functional impairment, as confirmed also by in vitro motility assay experiments. The enhanced carbonylation of the myofibrillar proteins observed in *Atg7* knockout muscles represents a posttranslational modification

apparently different from those induced by hydrogen peroxide at millimolar concentrations and described in Ref. 23, which induced an altered proportion of strongly bound cross bridges in relaxed conditions and not during contraction.

The fraction of strongly attached cross bridges in Akt-overexpressing muscles. The Akt/PKB kinase acts downstream of phosphatidylinositol 3-kinase and represents a critical signaling component of the anabolic pathways which are activated by various stimuli, including growth factors, mechanical stimuli, and insulin. Phospho-Akt finds a number of target proteins stimulating protein synthesis, cell survival, cell cycle, and metabolism and inhibiting protein breakdown. In particular, Akt/PKB stimulates the growth of skeletal muscle fibers in a mammalian target of rapamycin-dependent way and simultaneously downregulates the activity of FoxO transcription factors, which in turn activate ubiquitin-proteasome pathway and autophagy pathway (see Ref. 6 for a review). Overexpression of a constitutively active Akt was obtained by injecting tamoxifen every other day in Akt transgenic mice generated by crossing a transgenic line that expresses the Cre recombinase

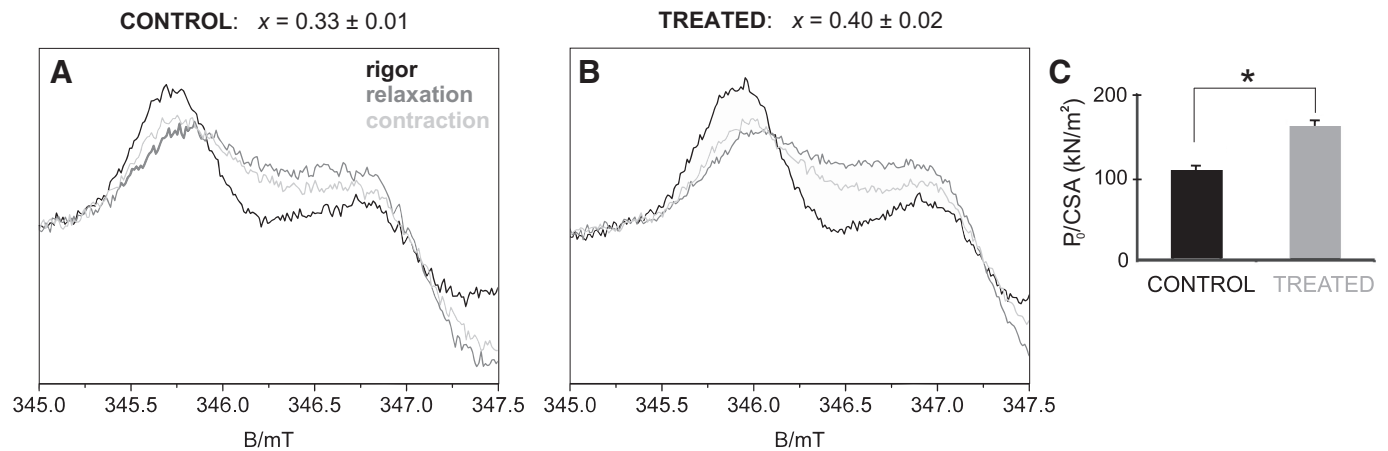


Fig. 5. *A*: continuous wave-electron paramagnetic resonance (CW-EPR) spectra at room temperature on mouse tibialis anterior control muscle in rigor (black), relaxation (gray), and contraction (light gray) state. *B*: CW-EPR spectra at room temperature on tamoxifen-treated mouse tibialis anterior muscle in rigor (black), relaxation (gray), and contraction (light gray) state. Values of the ratio x , indicating the proportion of strongly bound cross bridges are means \pm SD with $n = 20$ (equal number of bundles from 4 different animals, 2 males and 2 females, 5–6 mo old). * $P < 0.05$, significant difference (95% confidence). *C*: tension measurements performed at 20°C on single skinned fibers [Modified from Blaauw et al. (5), with permission from *The FASEB Journal* (www.fasebj.org).]

under a muscle-specific (myosin light chain 1 fast) promoter with a second line that expresses Akt1 only after the deletion of an upstream DNA sequence by the Cre recombinase (5). Tamoxifen treatment for 1 wk is sufficient to induce a large hypertrophy, which is limited to skeletal muscle. After 3 wk of treatment, mice show a 50% increase in mass (5) and a great increase in force generation, but tension measurements reveal that, after normalization to fibers cross-sectional area, hypertrophic muscles show a 47% increase in the contractile performance (Fig. 5C). Importantly, no change in fiber type accompanies the hypertrophic growth (5). We performed EPR experiments on these mice and compared our results with muscles of control animals of the same age and treated in the same way, except for the tamoxifen administration. Our results are shown in Fig. 5. All the results are presented as the means \pm SD calculated over all the repetitions. Significance is defined as a value of $P < 0.05$ (95% confidence). For the statistical analysis, all the considerations previously made for Atg7 held true in this case as well.

Significant differences in the fraction of strongly attached the cross bridges were detected between control and treated fiber bundles; in particular, we found $x = 0.33 \pm 0.01$ for the control and $x = 0.40 \pm 0.02$ for altered samples, correspond-

ing to a significant increase of 21% in the number of cross bridges in tamoxifen-treated muscles. Compared with a 47% increase in active tension observed in single muscle fibers, a significant increase by 21% in the fraction of attached bridges might suggest the contribution of other mechanisms. As shown by Blaauw and coworkers (5), the swelling that typically occurs during single fiber permeabilization was less pronounced in tamoxifen treated than in control fibers, likely due to some cytoskeleton remodeling. Thus the greater active tension could also find a partial explanation in this phenomenon. We considered, however, another possible reason, related to the difference among the preparations used for tension measurements, i.e., single permeabilized fibers, and for EPR spectra recording, i.e., bundles of several tens of fibers. Evidence in favor of the relevance of the structure of the bundles and of the fiber orientation is reported in Fig. 6.

In Fig. 6, *A* and *B*, the spectra in rigor state of fiber bundles from two different muscles (tibialis and psoas) from Akt-overexpressing mice are compared with their analogs from control mice. In both cases, it is possible to detect a rather pronounced presence of the parallel component in the perpendicular orientation mode of the sample cell (Fig. 1*B*), possibly

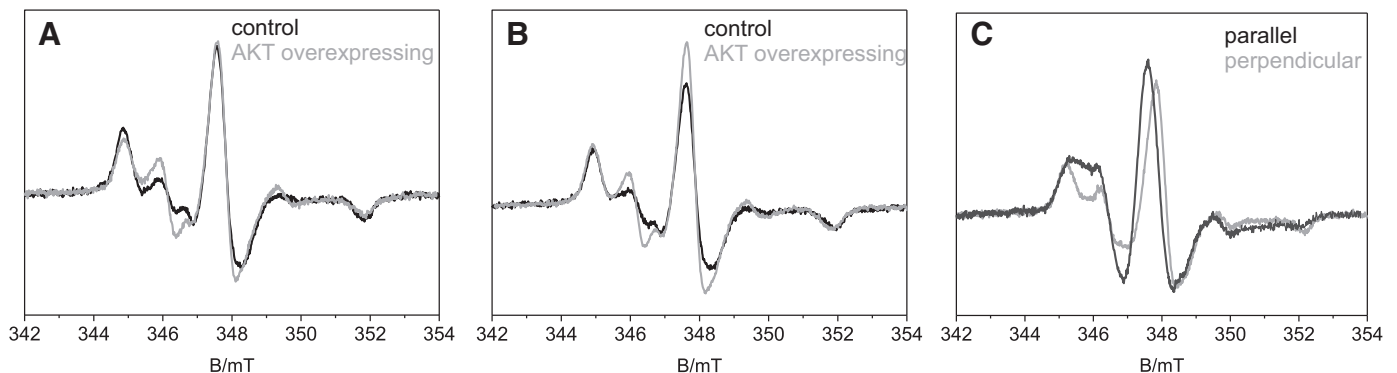


Fig. 6. *A*: continuous wave-electron paramagnetic resonance (CW-EPR) spectra at room temperature on psoas muscle of control (black) and Akt-overexpressing mice (gray) in rigor state. *B*: CW-EPR spectra at room temperature on tibialis muscle of control (black) and Akt-overexpressing mice (gray) in rigor state. *C*: orientation effect in spectra obtained on mouse gastrocnemius Akt-overexpressing muscle in perpendicular (gray) and parallel (black) mode in rigor state.

due to the intrinsic disorder of the myofibrils inside the fibers in the transgenic muscles. It is worth pointing out that the $2A_{zz}$ splitting in the perpendicular orientation is not significantly different from the rigid-limit value (10); therefore, in rigor state, the spectrum is sensitive only to the global orientation of myosin head and not to the rotation of the probe relative to the head. The remarkable difference in the EPR spectra of fibers oriented parallel or perpendicular with respect to the magnetic field suggests that, in the rigor state, the spin probe has a preferred orientational distribution relative to the fiber axis.

The consistent results in psoas and tibialis (Fig. 6, A and B) suggest that the disorder is not muscle (or even bundle) dependent, but it is an intrinsic characteristic due to the hypertrophic alteration of Akt-overexpressing muscles. The orientation selection, in fact, is not complete, leading to a mixture of parallel and perpendicular orientation of the fibers in the parallel orientation (Fig. 6C). For this reason, only very short bundles of fibers were analyzed in our study (4 mm) to carefully overcome this problem and extrapolate the correct proportion of strongly bound cross bridges.

In conclusion, the aim of our study was to shed light on the mechanisms responsible for the altered contraction performance in two models of genetically modified muscle fibers, by means of a multidisciplinary approach based on the comparison between EPR spectroscopic measurements and functional mechanical assays. Our results show that, both in the case of hypertrophic and atrophic muscles, an alteration occurs in the fraction of myosin heads that are strongly bound to actin during maximal isometric contraction. In the case of atrophic *Atg7* knockout muscles, in particular, the decrease of the proportion of attached cross bridges coincides with the decrease in tension on skinned fibers during contraction. This leads to the conclusion that the altered tension generation has to be ascribed to alteration in the number of strongly bound cross bridges with respect to control. Interestingly, the decrease in the fraction of attached cross bridges is less pronounced in aged muscles, and this is probably due to the fact that the control preparations in terms of contractile power are already compromised in old animals. Strong experimental evidence supports the view that oxidative posttranslational modifications of myosin are responsible for the reduction in cross bridge formation. In the case of hypertrophic Akt-overexpressing muscles, on the other hand, our results suggest that the increase in the contractile tension can be only partially described as an increase in the number of the strongly bound cross bridges between actin and myosin upon contraction, suggesting that some other factors have to be taken into account.

Finally, the results reported in this study confirmed that EPR spectroscopy coupled with functional assay provides a powerful tool to investigate the link between structural and functional adaptations of muscles to conditions, which induce either atrophy or hypertrophy.

ACKNOWLEDGMENTS

Present address of L. Galazzo: Faculty of Chemistry and Biochemistry, Ruhr-Universität Bochum, Universitätsstr, 150, 44801 Bochum, Germany (e-mail: laura.galazzo@rub.de).

GRANTS

This work was supported by the Cassa di Risparmio di Padova e Rovigo (CARIPARO) Foundation (M3PC project) by the Ministry of Education, Universities and Research (PRIN2010-2011 prot. 2010FM38P_004).

DISCLOSURES

No conflicts of interest, financial or otherwise, are declared by the authors.

AUTHOR CONTRIBUTIONS

C.R. and D.C. conceived and designed research; L.G., L.N., and F.L.V. performed experiments; L.G. and D.C. analyzed data; L.G., B.B., M.S., C.R., and D.C. interpreted results of experiments; L.G. prepared figures; L.G. and D.C. drafted manuscript; L.G., L.N., F.L.V., A.P., M.S., C.R., and D.C. edited and revised manuscript; L.G., A.P., B.B., M.S., C.R., and D.C. approved final version of manuscript.

REFERENCES

- Altenbach C, Flitsch SL, Khorana HG, Hubbell WL. Structural studies on transmembrane proteins. 2. Spin labeling of bacteriorhodopsin mutants at unique cysteines. *Biochemistry* 28: 7806–7812, 1989. doi:10.1021/bi00445a042.
- Altenbach C, Marti T, Khorana HG, Hubbell WL. Transmembrane protein structure: spin labeling of bacteriorhodopsin mutants. *Science* 248: 1088–1092, 1990. doi:10.1126/science.2160734.
- Barnett VA, Thomas DD. Resolution of conformational states of spin-labeled myosin during steady-state ATP hydrolysis. *Biochemistry* 26: 314–323, 1987. doi:10.1021/bi00375a044.
- Berliner LJ, Grunwald J, Hankovszky HO, Hideg K. A novel reversible thiol-specific spin label: papain active site labeling and inhibition. *Anal Biochem* 119: 450–455, 1982. doi:10.1016/0003-2697(82)90612-1.
- Blaauw B, Canato M, Agatea L, Toniolo L, Mammucari C, Masiero E, Abraham R, Sandri M, Schiaffino S, Reggiani C. Inducible activation of Akt increases skeletal muscle mass and force without satellite cell activation. *FASEB J* 23: 3896–3905, 2009. doi:10.1096/fj.09-131870.
- Blaauw B, Schiaffino S, Reggiani C. Mechanisms modulating skeletal muscle phenotype. *Compr Physiol* 3: 1645–1687, 2013. doi:10.1002/cphy.c130009.
- Bordignon E, Steinhoff HJ. Membrane protein structure and dynamics studied by site-directed spin labeling ESR. In: *ESR Spectroscopy in Membrane Biophysics*, edited by Hemminga MA, Berliner LJ. New York: Springer US, 2007, p. 129–164.
- Bruce SA, Phillips SK, Woledge RC. Interpreting the relation between force and cross-sectional area in human muscle. *Med Sci Sports Exerc* 29: 677–683, 1997. doi:10.1097/00005768-199705000-00014.
- Carnio S, LoVerso F, Baraibar MA, Longa E, Khan MM, Maffei M, Reischl M, Canepari M, Loeffler S, Kern H, Blaauw B, Friguet B, Bottinelli R, Rudolf R, Sandri M. Autophagy impairment in muscle induces neuromuscular junction degeneration and precocious aging. *Cell Rep* 8: 1509–1521, 2014. doi:10.1016/j.celrep.2014.07.061.
- Fajer PG, Fajer EA, Matta JJ, Thomas DD. Effect of ADP on the orientation of spin-labeled myosin heads in muscle fibers: a high-resolution study with deuterated spin labels. *Biochemistry* 29: 5865–5871, 1990. doi:10.1021/bi00476a031.
- Klare JP. Site-directed spin labeling EPR spectroscopy in protein research. *Biol Chem* 394: 1281–1300, 2013. doi:10.1515/hsz-2013-0155.
- Krivickas LS, Dorer DJ, Ochala J, Frontera WR. Relationship between force and size in human single muscle fibres. *Exp Physiol* 96: 539–547, 2011. doi:10.1113/expphysiol.2010.055269.
- Lowe DA, Surek JT, Thomas DD, Thompson LV. Electron paramagnetic resonance reveals age-related myosin structural changes in rat skeletal muscle fibers. *Am J Physiol Cell Physiol* 280: C540–C547, 2001. doi:10.1152/ajpcell.2001.280.3.C540.
- Lowe DA, Williams BO, Thomas DD, Grange RW. Molecular and cellular contractile dysfunction of dystrophic muscle from young mice. *Muscle Nerve* 34: 92–100, 2006. doi:10.1002/mus.20562.
- Masiero E, Agatea L, Mammucari C, Blaauw B, Loro E, Komatsu M, Metzger D, Reggiani C, Schiaffino S, Sandri M. Autophagy is required to maintain muscle mass. *Cell Metab* 10: 507–515, 2009. doi:10.1016/j.cmet.2009.10.008.
- Masiero E, Sandri M. Autophagy inhibition induces atrophy and myopathy in adult skeletal muscles. *Autophagy* 6: 307–309, 2010. doi:10.4161/auto.6.2.11137.
- Mitchell WK, Williams J, Atherton P, Larvin M, Lund J, Narici M. Sarcopenia, dynapenia, and the impact of advancing age on human skeletal muscle size and strength; a quantitative review. *Front Physiol* 3: 260, 2012. doi:10.3389/fphys.2012.00260.
- Murgia M, Toniolo L, Nagaraj N, Ciciliot S, Vindigni V, Schiaffino S, Reggiani C, Mann M. Single muscle fiber proteomics reveals fiber-type-

- specific features of human muscle aging. *Cell Rep* 19: 2396–2409, 2017. doi:10.1016/j.celrep.2017.05.054.
19. Musarò A, McCullagh K, Paul A, Houghton L, Dobrowolny G, Molinaro M, Barton ER, Sweeney HL, Rosenthal N. Localized Igf-1 transgene expression sustains hypertrophy and regeneration in senescent skeletal muscle. *Nat Genet* 27: 195–200, 2001. doi:10.1038/84839.
 20. Nogara L, Naber N, Pate E, Canton M, Reggiani C, Cooke R. Piperine's mitigation of obesity and diabetes can be explained by its up-regulation of the metabolic rate of resting muscle. *Proc Natl Acad Sci USA* 113: 13009–13014, 2016. doi:10.1073/pnas.1607536113.
 21. Ostap EM, Barnett VA, Thomas DD. Resolution of three structural states of spin-labeled myosin in contracting muscle. *Biophys J* 69: 177–188, 1995. doi:10.1016/S0006-3495(95)79888-5.
 22. Percario V, Boncompagni S, Protasi F, Pertici I, Pinzauti F, Caremani M. Mechanical parameters of the molecular motor myosin II determined in permeabilised fibres from slow and fast skeletal muscles of the rabbit. *J Physiol* 596: 1243–1257, 2018. doi:10.1113/JP275404.
 23. Prochniewicz E, Lowe DA, Spakowicz DJ, Higgins L, O'Connor K, Thompson LV, Ferrington DA, Thomas DD. Functional, structural, and chemical changes in myosin associated with hydrogen peroxide treatment of skeletal muscle fibers. *Am J Physiol Cell Physiol* 294: C613–C626, 2008. doi:10.1152/ajpcell.00232.2007.
 24. Sale K, Sár C, Sharp KA, Hideg K, Fajer PG. Structural determination of spin label immobilization and orientation: a Monte Carlo minimization approach. *J Magn Reson* 156: 104–112, 2002. doi:10.1006/jmre.2002.2529.
 25. Salviati G, Sorenson MM, Eastwood AB. Calcium accumulation by the sarcoplasmic reticulum in two populations of chemically skinned human muscle fibers. Effects of calcium and cyclic AMP. *J Gen Physiol* 79: 603–632, 1982. doi:10.1085/jgp.79.4.603.
 26. Schiaffino S, Dyar KA, Ciciliot S, Blaauw B, Sandri M. Mechanisms regulating skeletal muscle growth and atrophy. *FEBS J* 280: 4294–4314, 2013. doi:10.1111/febs.12253.
 27. Seidel JC, Chopek M, Gergely J. Effect of nucleotides and pyrophosphate on spin labels bound to S1 thiol groups of myosin. *Biochemistry* 9: 3265–3272, 1970. doi:10.1021/bi00818a021.
 28. Staron RS, Hagerman FC, Hikida RS, Murray TF, Hostler DP, Crill MT, Ragg KE, Toma K. Fiber type composition of the vastus lateralis muscle of young men and women. *J Histochem Cytochem* 48: 623–629, 2000. doi:10.1177/002215540004800506.
 29. Stelzer JE, Widrick JJ. Effect of hindlimb suspension on the functional properties of slow and fast soleus fibers from three strains of mice. *J Appl Physiol* (1985) 95: 2425–2433, 2003. doi:10.1152/japplphysiol.01091.2002.
 30. Thomas DD, Cooke R. Orientation of spin-labeled myosin heads in glycerinated muscle fibers. *Biophys J* 32: 891–906, 1980. doi:10.1016/S0006-3495(80)85024-7.
 31. Thomas DD, Ramachandran S, Roopnarine O, Hayden DW, Ostap EM. The mechanism of force generation in myosin: a disorder-to-order transition, coupled to internal structural changes. *Biophys J* 68, Suppl 4: 135S–141S, 1995.
 32. Trappe T, Williams R, Carrithers J, Raue U, Esmarck B, Kjaer M, Hickner R. Influence of age and resistance exercise on human skeletal muscle proteolysis: a microdialysis approach. *J Physiol* 554: 803–813, 2004. doi:10.1113/jphysiol.2003.051755.

